Ionic and electronic structures of liquid aluminium from the quantal hypernetted-chain equations combined with the molecular dynamics method

1994 J. Phys.: Condens. Matter 6 10221

(http://iopscience.iop.org/0953-8984/6/47/005)

J. Phys.: Condens. Matter 6 (1994) 10221–10236. Printed in the UK

Ionic and electronic structures of liquid aluminium from the quantal hypernetted-chain equations combined with the molecular dynamics method

J Chihara† and S Kambayashi‡

† Solid State Physics Laboratory, Japan Atomic Energy Research Institute, Tokai, Ibaraki 319-11, Japan

‡ Computing and Information Systems Centre, Japan Atomic Energy Research Institute, Tokai, Ibaraki 319-11, Japan

Received 12 July 1994, in final form 31 August 1994

Abstract. Liquid aluminium is a simple metal which can be modelled as an electron–ion mixture with pairwise interparticle interactions. On the basis of the density functional theory, the quantal hypernetted-chain (QHNC) formulation for the electron–ion mixture provides exact expressions for the electron–ion and ion–ion radial distribution functions (RDF), and shows that this electron–ion mixture can be treated as a quasi-one-component liquid interacting only through a pairwise interaction without many-body forces. Using the approximation that the exchange–correlation effect of the conduction electrons in the mixture is represented by the local-field correction (LFC) of the jellium model, the QHNC formulation offers a procedure for performing a first-principles molecular dynamics (MD) simulation where the effective ion–ion interaction is determined self-consistently with its liquid structure.

Using the Geldart–Vosko (GV) LFC, the structure factor of liquid aluminium near its melting point is calculated by this procedure (QHNC–MD) and is in fairly good agreement with experiment, in conjunction with the bridge function and the direct correlation function. The calculated ion–ion RDF exhibits a significant dependence on which kind of LFC is adopted in the QHNC–MD method in contrast with what is found in the case of liquid alkali metals where the LFC of the GV type and of the local-density-approximation type yield almost the same structure factors. The effective ion–ion potential from the QHNC–MD method with the GV LFC becomes a deep negative well where the potential of Dagens, Geldart and Taylor has a positive minimum. The electron–ion RDF is obtained in a consistent way with the density profile $\rho(r)$ of a neutral pseudoatom. The Ashcroft model potential with core radius $r_c = 1.12a_B$ produces an electron density distribution $\rho(r)$ and ion–ion RDF almost identical with the QHNC–MD results.

1. Introduction

Liquid aluminium is considered as a simple metal, like alkali liquid metals, in that the core electrons forming an ion can be clearly distinguished from the valence electrons and that the ion-core electrons do not overlap with those of neighbouring ions significantly. Hence, a simple metal can be regarded as a mixture of electrons and ions interacting via pair potentials among them: the ions behave as a classical fluid and the free electrons form a quantum fluid (referred to as the electron–ion model). Previously, we have derived exact expressions for the ion–ion and electron–ion radial distribution functions (RDF) on the basis of the density functional theory applied to the electron–ion model, and the quantal hypernetted-chain (QHNC) equations are derived by introducing some approximations to

0953-8984/94/4710221+16$19.50

these exact expressions [1–4]. In the QHNC formulation, the effective interatomic potential $v^{\mathrm{eff}}(r)$ is determined to be consistent with the density distribution $\rho(r)$ of a pseudoatom, and the ion–ion and electron–ion RDFs at the same time. The non-linear effect in the electron screening is taken into account automatically by the density functional method in such a way that the non-linear pseudopotential is constructed in terms of the electron–ion direct correlation function (DCF) $C_{\mathrm{eI}}(r)$. Only the atomic number Z_{A} is needed to proceed with this calculation, as is the case for the calculation of the atomic structure. Furthermore, the QHNC equations have been shown to give ionic and electronic structures in excellent agreement with experiment when applied to alkali metals (Li, Na and K) [3, 5, 6].

However, there are three conduction electrons per atom in a liquid aluminium, while alkali liquid metals have only one conduction electron per atom. In the present work, we try to apply this QHNC formulation to aluminium liquid anticipating that we may find some differences from alkali metals, although it also constitutes a simple metal. In the standard approach, a liquid metal is considered as a quasi-one-component liquid with an effective potential determined by a proper pseudopotential using the second-order perturbation. There are many calculations of the liquid structure for aluminium which follow this approach [7]–[10], but their agreement with experiment is not as good as for alkali metals when calculated without the adjusting procedure. In this standard approach, even when the pseudopotential is determined from first principles, computer simulations such as the MD using the effective interatomic potential based on this pseudopotential cannot be considered as first-principles calculations since many-body forces coming from higher-order terms in perturbation theory are ignored; these many-body interactions become important even for a alkali metal. Hafner and Jank [10] calculated an effective interaction for liquid aluminium on the basis of the first-principles optimized pseudopotential developed by Harrison, and performed the MD simulation to obtain the RDF or the structure factor, obtaining fairly good agreement with one of the experiments by adjusting the parameter α in the Xα exchange potential; without this adjustment, their result deviates from the experiment noticeably. In their treatment, the non-linear effect arising from the neglected higher-order terms in perturbation theory is not clearly analysed. On the other hand, Dagens, Rasolt and Taylor (DRT) [11] constructed a first-principles non-linear pseudopotential, which yields an effective pairwise potential taking account of many-body force effect, and with this potential Jacucci *et al* calculated the structure factor of Al by means of the MD simulation; it also does not agree so well with experiments, compared with the case of alkali metals. At this stage it is not clear whether these discrepancies are due to inaccuracy in the experiments or due to problems on the theoretical side. At least, it is not certain which structure factor data set is most reliable for comparison with theoretical results, since the data obtained by the many investigators show a wide divergence. In the present work, the QHNC formulation is applied to a liquid aluminium using the same approximation as was adopted in the case of liquid alkali metals, where we obtained results showing excellent agreement with experiment.

2. Formulation

A liquid metal can be thought of as 'simple' if the free electrons are clearly distinguished from the bound electrons forming an ion core and if the ions and electrons in it are interacting with each other via pairwise potentials $v_{ij}(r)$. In the ion–electron mixture, the radial distribution functions $g_{\mathrm{II}}(r)$ for the ions are identical with the inhomogeneous electron or ion density distribution $n_i(r|\mathrm{I})$ around a fixed ion in the mixture—that is, the density distributions $n_i(r|\{U_\alpha = v_{\alpha\mathrm{I}}\})$ (i = I or e) under external potentials, $\{U_\alpha(r) = v_{\alpha\mathrm{I}}(r)\}$, caused by the ion fixed at the origin. As a consequence, the density functional theory can

lead to exact expressions for $n_i(r|\{U_\alpha = v_{\alpha I}\})$ (i = I or e) in terms of density distributions $n_i^0(r|U_i^{\text{eff}})$ of non-interacting systems under such effective potentials $U_i^{\text{eff}}(r)$ as to yield $n_i^0(r|U_i^{\text{eff}}) \equiv n_i(r|U_I U_e)$. In this way, the DF theory provides *exact*, although formal, expressions for the RDFs $g_{iI}(r)$ for ions as follows [4, 12]:

$$g_{iI}(r) = n_i^0(r|U_i^{\text{eff}})/n_0^i \tag{1}$$

$$U_i^{\text{eff}}(r) \equiv v_{iI}(r) - \frac{1}{\beta}\sum_\ell \int C_{i\ell}(|r - r'|)\, n_0^\ell [g_{\ell I}(r') - 1]\, dr' - B_{iI}(r)/\beta \tag{2}$$

in terms of the DCFs $C_{ij}(r)$ and bridge functions $B_{iI}(r)$. In relation to the above equations, the Ornstein-Zernike (OZ) relations in the ion–electron mixture are written as

$$g_{II}(r) - 1 = C_{II}(r) + \Gamma_{II}(r) \tag{3}$$

$$g_{eI}(r) - 1 = \hat{B}C_{eI}(r) + \hat{B}\Gamma_{eI}(r) \tag{4}$$

with

$$\Gamma_{ij}(r) \equiv \sum_\ell \int C_{i\ell}(|r - r'|)\, n_0^\ell [g_{\ell j}(r') - 1]\, dr' \tag{5}$$

where $\hat{B}$ denotes an operator defined by

$$\mathcal{F}_Q[\hat{B}^\alpha f(r)] \equiv (\chi_Q^0)^\alpha \int e^{iQ\cdot r} f(r)\, dr$$

for an arbitrary real number α, and represents a quantum effect of the electrons through the density response function χ_Q^0 of the non-interacting electrons. In the usual approach, a liquid metal is regarded as a quasi-one-component fluid with an effective interatomic interaction $v^{\text{eff}}(r)$. From this point of view, the effective interaction $v^{\text{eff}}(r)$ can be defined in such a way that the RDF $g(r)$ of the one-component system modelled as a liquid metal should be identical to $g_{II}(r)$ in the mixture given by (1):

$$g(r) = \exp[-\beta v^{\text{eff}}(r) + \gamma(r) + B(r)] \equiv g_{II}(r) \tag{6}$$

with

$$\gamma(r) \equiv \int C(|r - r'|)\, n_0^I [g(r') - 1]\, dr' . \tag{7}$$

Here, the one-component DCF $C(Q)$ is related to the ion–ion DCF $C_{II}(Q)$ of the mixture via

$$C(Q) = C_{II}(Q) + \frac{|C_{eI}(Q)|^2 n_0^e \chi_Q^0}{1 - n_0^e C_{ee}(Q)\chi_Q^0} \tag{8}$$

since it is defined as $n_0^I C(Q) \equiv 1 - 1/S_{II}(Q)$. Therefore, it is shown from the definition (6) with the help of (8) that the effective potential $v^{\text{eff}}(Q)$ can be expressed exactly as

$$\beta v^{\text{eff}}(Q) \equiv \beta v_{II}(Q) - \frac{|C_{eI}(Q)|^2 n_0^e \chi_Q^0}{1 - n_0^e C_{ee}(Q)\chi_Q^0} \tag{9}$$

when the bridge function $B(r)$ of the one-component system is taken to be $B_{II}(r)$ for the mixture.

The integral equations for $g_{II}(r)$ and $g_{eI}(r)$, (1) coupled with (3) and (4), are rewritten as the equation for the DCFs:

$$C(r) = \exp[-\beta v^{\text{eff}}(r) + \gamma(r) + B_{II}(r)] - 1 - \gamma(r) \tag{10}$$

$$\hat{B}C_{eI}(r) = n_e^0(r|\tilde{v}_{eI} - \Gamma_{eI}/\beta - B_{eI}/\beta)/n_0^e - 1 - \hat{B}\Gamma_{eI}(r) . \tag{11}$$

This set of equations, (10) and (11), constitute a set of integral equations for determining the RDFs in the ion–electron model, if $C_{ee}(r)$, $B_{el}(r)$, $B_{II}(r)$, $v_{II}(r)$ and $v_{el}(r)$ are given beforehand. The first equation (10) becomes an integral equation for the RDF, $g(r)$, of the quasi-one-component liquid with the interaction $v^{eff}(r)$ specified by (9). On the other hand, the second equation (11) generates the pseudopotential $w_b(r) = -C_{el}(Q)/\beta$, evaluating $v^{eff}(r)$ by (9) in conjunction with the RDF $g(r)$, which is to be obtained beforehand from the first equation (10). These two equations constitute a coupled set of integral equations for determining the RDFs and the effective interactions $v^{eff}(r)$. In this sense, the effective interatomic potential in the QHNC formulation depends on the liquid structure through the RDF $g_{II}(r)$, in contrast with usual effective interatomic potentials for liquid metals. Moreover, we note that these expressions indicate an important fact—that a liquid metal can be *exactly* described as a one-component fluid interacting only via *pairwise* interaction, without introducing a many-body potential to evaluate the RDF $g_{II}(r)$, if the ion–ion interaction $v_{II}(r)$ and the electron–ion interaction $v_{el}(r)$ in the ion–electron mixture are pairwise.

In the simple liquid metal, (a) the electron–electron DCF $C_{ee}(Q)$ can be approximated by the LFC $G^{jell}(Q)$ of the jellium model in the form: $C_{ee}(Q) = -\beta v_{ee}(Q)(1 - G^{jell}(Q))$, by neglecting the ion configuration effect on the LFC $G(Q)$ of the mixture. This approximation also gives the formula for the effective potential in the form

$$\beta v^{eff}(Q) \equiv \beta v_{II}(Q) - |C_{el}(Q)|^2 n_0^e \chi_Q \tag{12}$$

with the density–density response function $\chi_Q \equiv \chi_Q^0/[1 + n_0^e \beta v_{ee}(Q)(1 - G^{jell}(Q))\chi_Q^0]$ of the electron in the jellium model, where the ions are replaced by the uniform positive background.

In addition, the electron–ion correlation in a simple metal is so weak that (b) the electron–ion bridge function $B_{el}(r)$ is neglected: $B_{el}(r) = 0$. By regarding a liquid metal with the atomic number Z_A as a mixture of nuclei and electrons [2], we have derived (c) the approximate bare electron–ion potential $\tilde{v}_{el}(r)$ in the form

$$\tilde{v}_{el}(r) = -Z_A e^2/r + \int v_{ee}(|r - r'|) n_e^b(r')\, dr' + \mu_{XC}(n_e^b(r) + n_0^e) - \mu_{XC}(n_0^e). \tag{13}$$

Here $n_e^b(r)$ denotes the bound-electron distribution, and $\mu_{XC}(n)$ is the exchange–correlation potential in the local-density approximation (LDA).

Now, equation (11) can determine the pseudopotential $-C_{el}(Q)/\beta$ under the approximations (a)–(c), if (d) the ion–ion bare potential $v_{II}(r)$ is taken as Coulombic: $v_{II}(r) = (Z_I e)^2/r$. When the effective interaction is given by (12) in this way, we can produce the RDF $g_{II}(r)$ from (10). In this formulation, the effective interatomic interaction $v^{eff}(r)$ is dependent on the RDF to be determined afterwards, since the pseudopotential is generated by (11), involving $g_{II}(r)$. From another point of view, this formulation suggests that we can perform an *ab initio* molecular dynamics simulation based on a *pairwise* interaction (12) to obtain the ion–ion RDF, which is used again as the input to achieve a pseudopotential leading to a new effective interatomic potential $v^{eff}(r)$; this process should be repeated to arrive at a convergence. In principle, we can obtain the RDF $g_{II}(r)$ and the ion–ion bridge function $B_{II}(r)$ by MD simulation in this way.

As an alternative to the MD simulation, we can set up the modified hypernetted chain (HNC) equation [13] from (10), with the additional approximation that (e) the ion–ion bridge function $B_{II}(r)$ in (10) is replaced by $B_{PY}(r; \eta)$ of the Percus–Yevick equation for hard spheres with diameter σ: $B_{II}(r) \simeq B_{PY}(r; \eta)$ with a packing fraction parameter defined by

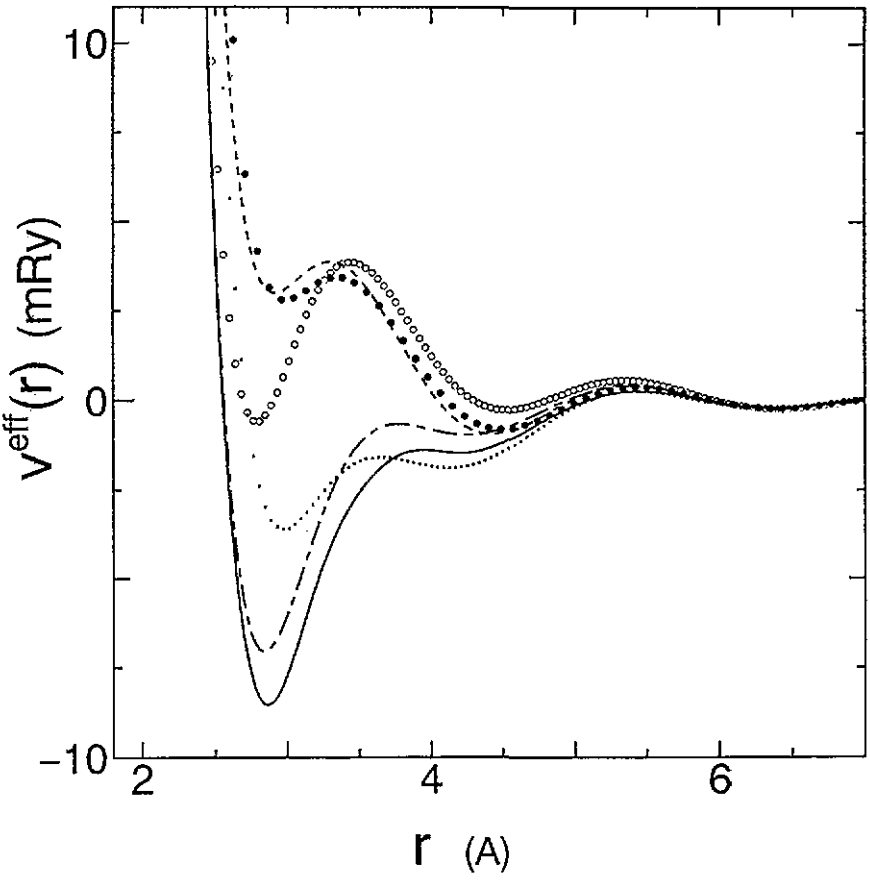

Figure 1. Effective ion–ion interactions for liquid aluminium. The DRT potential (full circles) is close to the Ashcroft-LDA potential (dashed curve), while the JV-LDA potential (open circles) becomes negative at the first minimum where the DRT potential has a positive minimum. The Ashcroft-GV, JV-GV and QHNC-GV potentials are denoted by the dotted, the chain and the full curves, respectively.

$\eta \equiv \pi n_0^1 \sigma^3/6$. Here, η is determined by the following condition:

$$\frac{1}{2} n_0^1 \int [g(r) - g_{PY}(r;\eta)] \frac{\partial B_{PY}(r;\eta)}{\partial \eta} \, dr + \frac{2\eta^2}{(1-\eta)^3} = 0 \tag{14}$$

which was proposed by Rosenfeld as the variational modified hypernetted-chain (VMHNC) equation [14].

It is very time consuming to apply the MD simulation in the determination of the RDF at each step of deriving the new effective potential from (12). It should be noticed that in a simple metal the effective interatomic potential is almost independent of its structure; even the approximation wherein the RDF $g_{II}(r)$ in $v_{el}^{eff}(r)$ of (2) is replaced by a step function provides a good description for $v^{eff}(r)$. Hence, at the beginning of our calculation, the VMHNC equation is repeatedly solved to achieve a self-consistent RDF $g_{II}(r)$ and the effective interaction $v^{eff}(r)$ using (10) and (11), instead of the MD simulation and (11). As the final step, this effective potential from the VMHNC equation is used for the MD simulation to get the RDF $g_{II}(r)$.

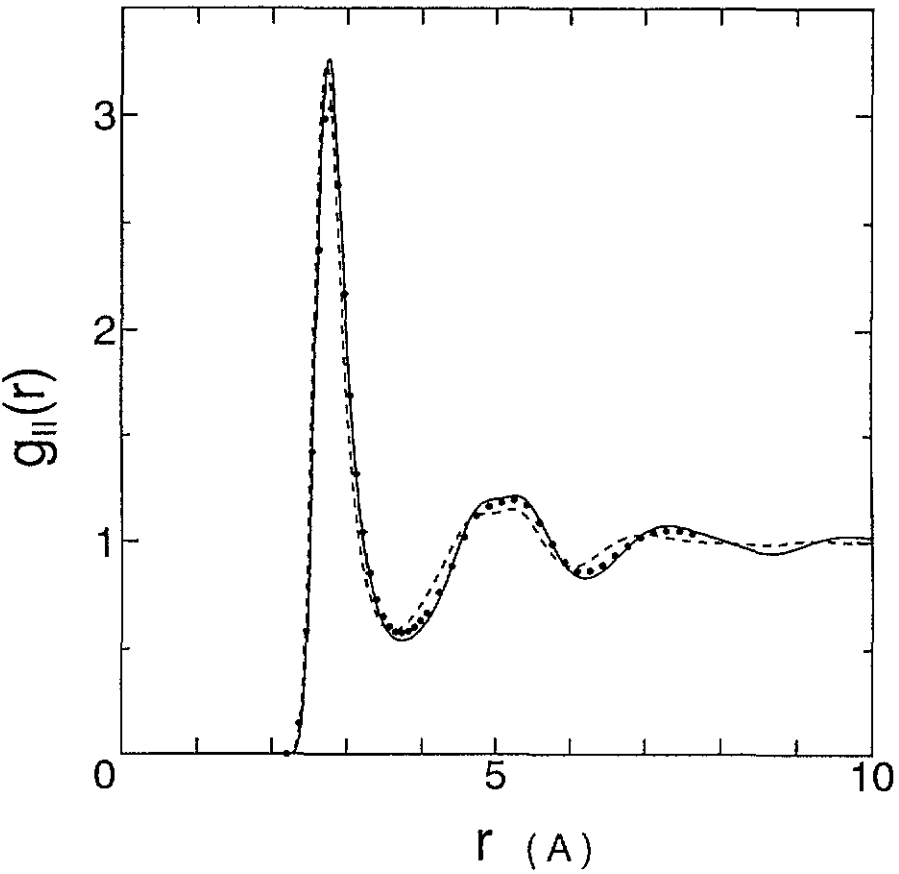

Figure 2. The comparison of the ion–ion RDF $g_{II}(r)$ for various effective potentials. The DRT $g_{II}(r)$ (full circles) is rather closer to the IV-GV $g_{II}(r)$ (full curve) than to the Ashcroft-LDA $g_{II}(r)$ (dashed curve), despite of the fact that the DRT effective potential is close to the Ashcroft-LDA potential.

3. Calculation procedure and results

When we proceed to apply this formulation to the liquid metal aluminium, it is necessary to introduce explicit expressions for the LDA $\mu_{XC}(n)$ and LFC $G^{jell}(Q)$ in the jellium model. There are many types of LFC calculated for the jellium model, where we have some knowledge of the conditions to be fulfilled. However, to date we have no criterion on the basis of which to judge beforehand which LFC is better for the evaluation of $v^{eff}(r)$, since the LFC in (9) is not that of the jellium model, but is that of the electron–ion mixture; this LFC depends on the ion configuration, which is replaced by the uniform positive background in the jellium model. In this calculation, we choose the LFC $G^{jell}(Q)$ to be that of Geldart and Vosko (GV) [15]:

$$G^{jell}(Q) = q^2/(2q^2 + 4g) \tag{15}$$

with $q = Q/Q_F$, $g = 1/(1+0.0155\alpha\pi r_s)$, $\alpha = (4/9\pi)^{1/3}$ and $r_s = (3/4\pi n_0^I)^{1/3}$ in units of the Bohr radius a_B and the Fermi wavevector Q_F, since the GV LFC has a simple expression, and has been applied to liquid alkali metals to produce results in excellent agreement with

experiments. Next, the exchange–correlation potential μ_{XC} involved in the bare electron–ion interaction $\tilde{v}_{el}(r)$ of (19) is taken to be that proposed by Gunnarsson and Lundqvist [16]:

$$\mu_{XC}(r_s) = -\frac{2}{\pi\alpha r_s}[1 + 0.0545 r_s \ln(1 + 11.4/r_s)] \text{ Ryd.} \tag{16}$$

With these approximations, which were adopted to calculate the liquid structure of alkali metal with success, the effective interatomic interaction $v^{eff}(r)$ and the RDF $g_{II}(r)$ are calculated self-consistently for liquid aluminium in practice.

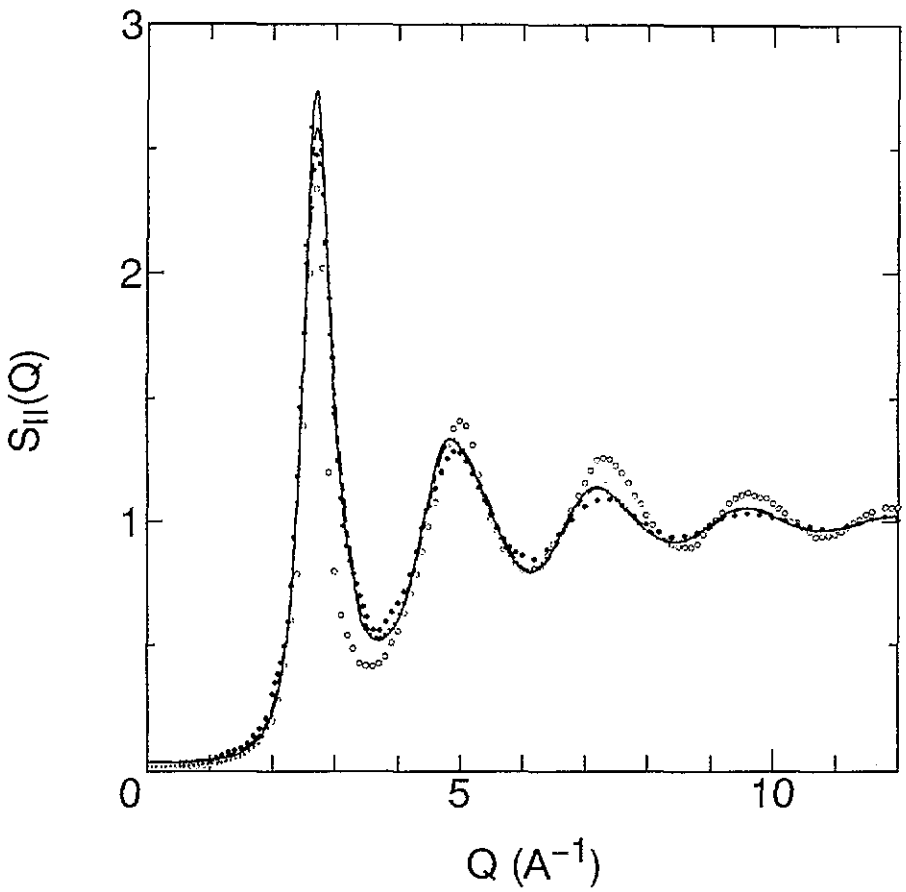

Figure 3. Structure factors calculated for various effective ionic potentials: the QHNC-GV (full curve), JV-GV (chain curve) and Ashcroft-GV (dotted curve) potentials, which are compared with the x-ray (full circles) and the neutron scattering (open circles) experiments.

At the first step, it is necessary to set up the initial $v^{eff}(r)$ for the beginning of the iteration to solve the QHNC equations; this is done by approximating $g_{II}(r)$ by a step function $\theta(r-a)$, with a the Wigner–Seitz radius, in addition to making the approximation $C_{el}(r) \simeq Z_I e^2/r$ in (2). These two approximations reduce the set of integral equations, (11) and (2), to the simple problem of calculating the electron density distribution around a fixed nucleus in the centre of spherical vacancy in the jellium: we refer to this as the jellium vacancy (JV) model. Next, the VMHNC equation is repeatedly solved to obtain the self-consistent ion–ion RDF for each new interatomic potential, which is determined by (12) in terms of

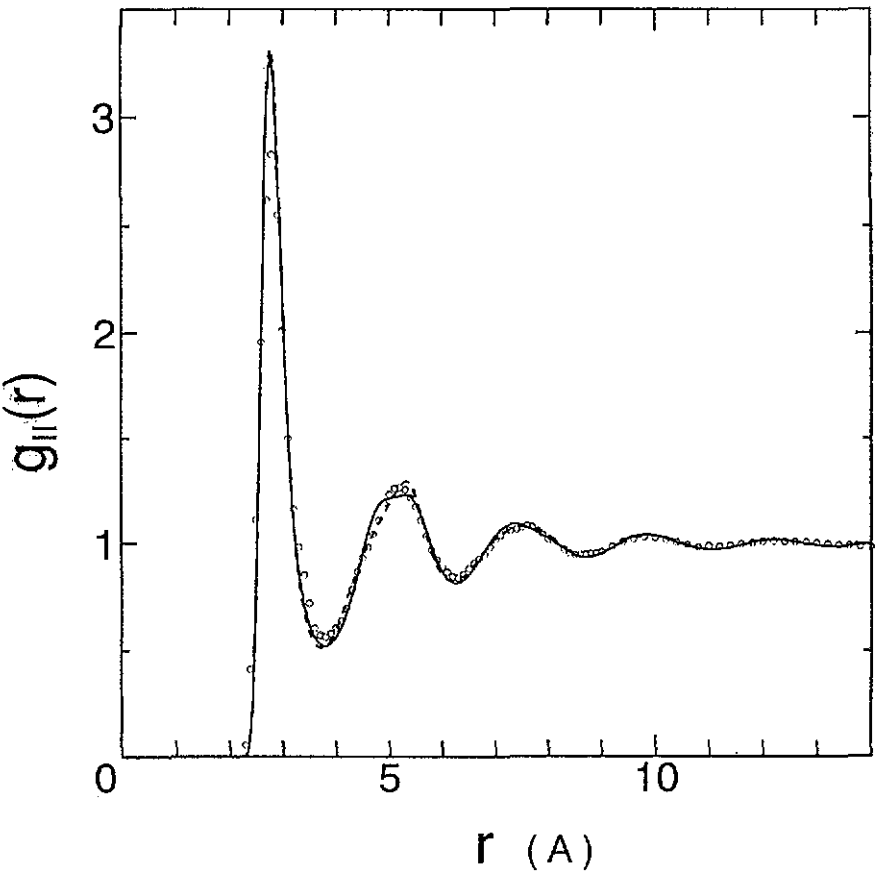

Figure 4. The comparison of the ion–ion RDF from the QHNC–MD method (full curve) with the experiment (open circles); the VMHNC result is shown by the dashed curve.

the electron–ion DCF from (11) for each ion–ion RDF. As the last step, the self-consistent interatomic potential obtained in this process is used for the MD simulation to get the RDF $g_{II}(r)$.

In order to perform the MD simulation, the interatomic potential must be truncated at the proper distance and the system size is taken to be some finite size. In the case of a liquid metal which has a long-range Friedel oscillation, this treatment may introduce an error in the RDF due to truncation. Furthermore, the RDF information is limited only to the region where the distance r is smaller than $L/2$, half of the side length L of the simulation cell; thus, it is necessary to extrapolate the RDF over the whole range to get the structure factor $S_{II}(Q)$ from the MD result. We have introduced a precise method for obtaining the RDF everywhere for the full potential $v^{\text{eff}}(r)$ from the MD result for the truncated potential:

$$u_c(r) \equiv \begin{cases} v^{\text{eff}}(r) - v^{\text{eff}}(R_c) & \text{for } r < R_c \\ 0 & \text{for } r \geqslant R_c\,. \end{cases} \tag{17}$$

This method is based on the fact that the bridge function is not sensitive to the long-range part of the potential. Using the HNC scheme for extrapolation of the MD RDF $g_{MD}(r)$ over

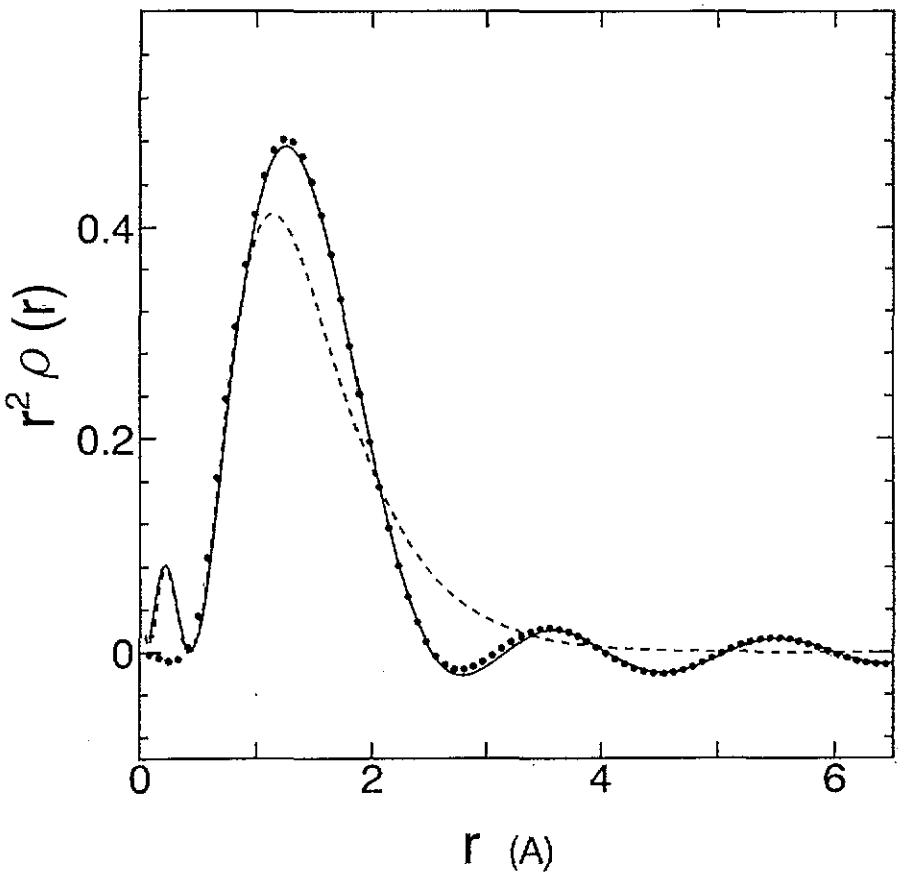

Figure 5. The electron density distribution $\rho(r)$ of a neutral pseudoatom calculated by the QHNC method (full curve) and the Ashcroft model potential (full circles); the dashed curve denotes the 3s-electron density distribution in a free aluminium atom.

the whole range for the cut-off potential $u_c(r)$:

$$g(r) \equiv \begin{cases} g_{MD}(r) & \text{for } r < R \\ \exp[-\beta u_c(r) + \gamma(r)] & \text{for } r \geqslant R \end{cases} \tag{18}$$

we can extract the bridge function $B_{MD}(r)$ for the cut-off potential; this bridge function was found to remain almost same even if the potential cut-off R_c was taken as very large. Thus, by assuming that the bridge function of a real system is approximated by $B_{MD}(r)$ obtained from the MD with low cut-off of the potential, the RDF of the full potential $v^{eff}(r)$ can be calculated from the MHNC equation combined with this bridge function. To get the correct bridge function from the small-size MD, it is important to take the extrapolating distance R as short as three or four interatomic spacings, discarding the RDF data beyond that distance. By applying the isokinetic constraint [17], the MD simulations have been performed for 4000 particles with potential truncated at $R_c = 5.31a$ over 10^5 time steps; the extrapolation distance is taken as $R = R_c$, although we have the RDF information up to $L/2 = 12.8a$ for this system size. The details of this procedure are described in [18].

The state of liquid aluminium under consideration is at the temperature 946 K and density $n_0^I = 5.298$ ions cm^{-3}, which is characterized by two parameters: the plasma

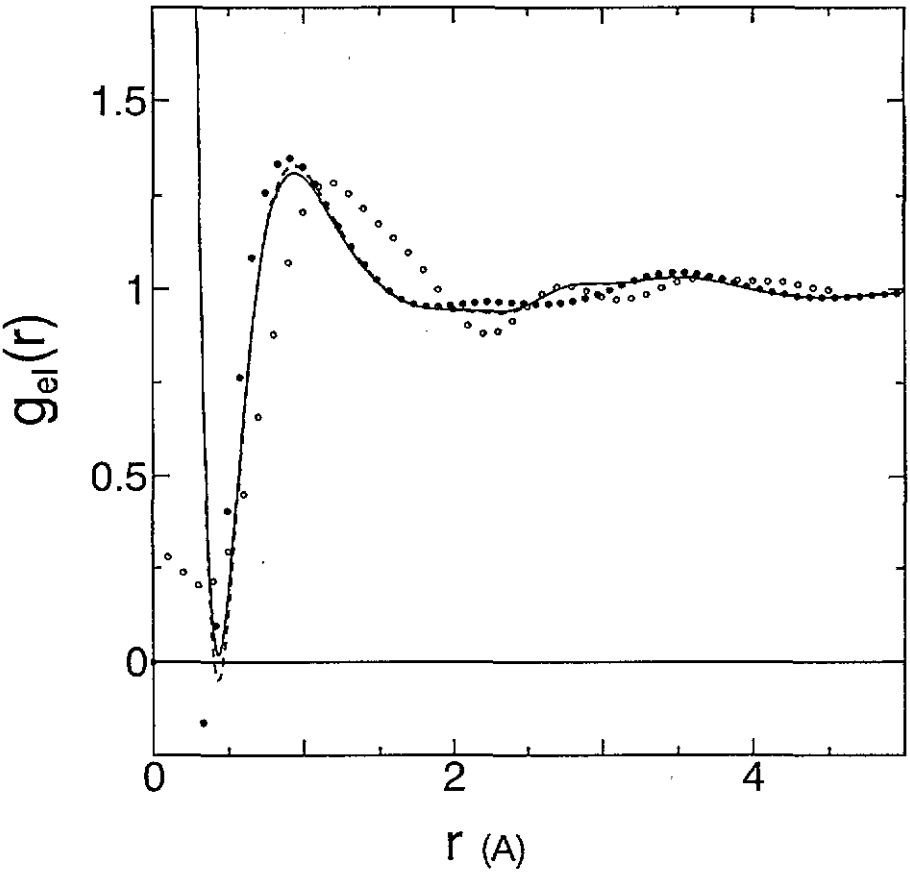

Figure 6. The electron–ion RDFs calculated by the QHNC method (full curve), the neutral pseudoatom method (dashed curve) and the Ashcroft model potential (full circles). The open circles are the experimental results obtained by Takeda *et al.*

parameter $\Gamma = 965.6$ and the electron sphere radius $r_s = 2.164$ in units of the Bohr radius a_B. In figure 1, the self-consistent effective potential (full curve) of liquid aluminium is plotted together with several other potentials; this aluminium potential is calculated from the QHNC equations combined with the VMHNC condition (14) to determine η. It is well known that the effective potential for aluminium is significantly dependent on what kind of LFC $G(Q)$ we choose for $\chi(Q)$ in (12). For comparison, we calculated the effective potential using the LFC of LDA type: $G(Q) = \gamma Q^2$, which is commonly used to calculate aluminium potentials. Here, we take $\gamma = 1/(4gQ_F^2)$, relevant to (15): $\gamma \equiv G(Q)/Q^2|_{Q=0}$. The JV method for calculating $v^{\text{eff}}(r)$ is shown to be identical to the neutral-pseudoatom method of Perrot [19, 20], and it is also essentially same as the DRT method, except as regards the important point that the non-local pseudopotential with fitting parameters is used in their formulation instead of the local pseudopotential $w_b(Q)$. The JV potential with the LDA $G(Q)$ (abbreviated as the JV-LDA, hereafter) becomes negative where the DRT potential shows a positive minimum near 3 Å. We remark that Perrot's potential is also negative there, similarly. The potential from the Ashcroft pseudopotential with core radius $r_c = 1.12a_B$ becomes very close to the DRT potential if the LFC is taken to be of LDA type. On the other hand, the minima of the potentials become deeply negative when the LFC of

GV (15) is adopted in the calculation of the QHNC, JV and Ashcroft potentials.

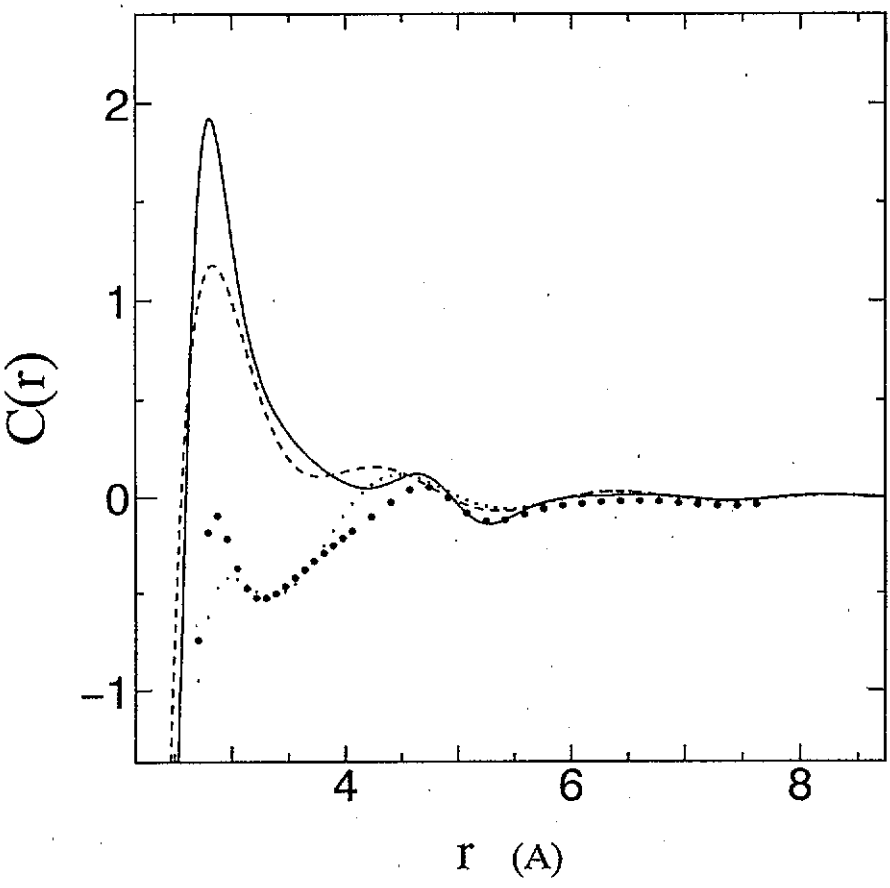

Figure 7. The direct correlation function (full curve) for the JV-GV potential (dashed curve) in comparison with the DCF (full circles) for the DRT potential (dotted curve).

It is interesting to notice in figure 2 that, although the Ashcroft and DRT potentials are close to each other, the MD RDF [21] of the DRT potential shows a large deviation from that calculated by MD using the Ashcroft potential with the LDA $G(Q)$ (Ashcroft-LDA), and that it agrees rather well with the MD result for the JV-GV potential. The RDF for the JV-GV potential becomes almost identical to those for the Ashcroft-GV and QHNC-GV potentials; the GV $G(Q)$ yields almost the same RDF whichever method of determining the pseudopotential is adopted among the QHNC, JV or Ashcroft approaches, as is the case for the LDA $G(Q)$. In alkali liquid metals, it does not cause any significant difference in the RDF whether one uses the LDA or GV $G(Q)$, although their effective potentials are quite different. In contrast with what is found for liquid alkali metals, the RDF (or the structure factor) of liquid aluminium depends significantly on the choice of the LFC to be used for χ_Q in (12). The structure factor (SF) is calculated by Fourier transformation of the MD RDF, which is corrected for a full potential and extrapolated over the whole range by the method mentioned above. The QHNC–MD SF is compared with the results of the x-ray [22] and neutron diffraction [23] experiments in figure 3, showing a fairly good agreement with the x-ray SF. However, the agreement between theoretical and experimental results is better in the case of alkali

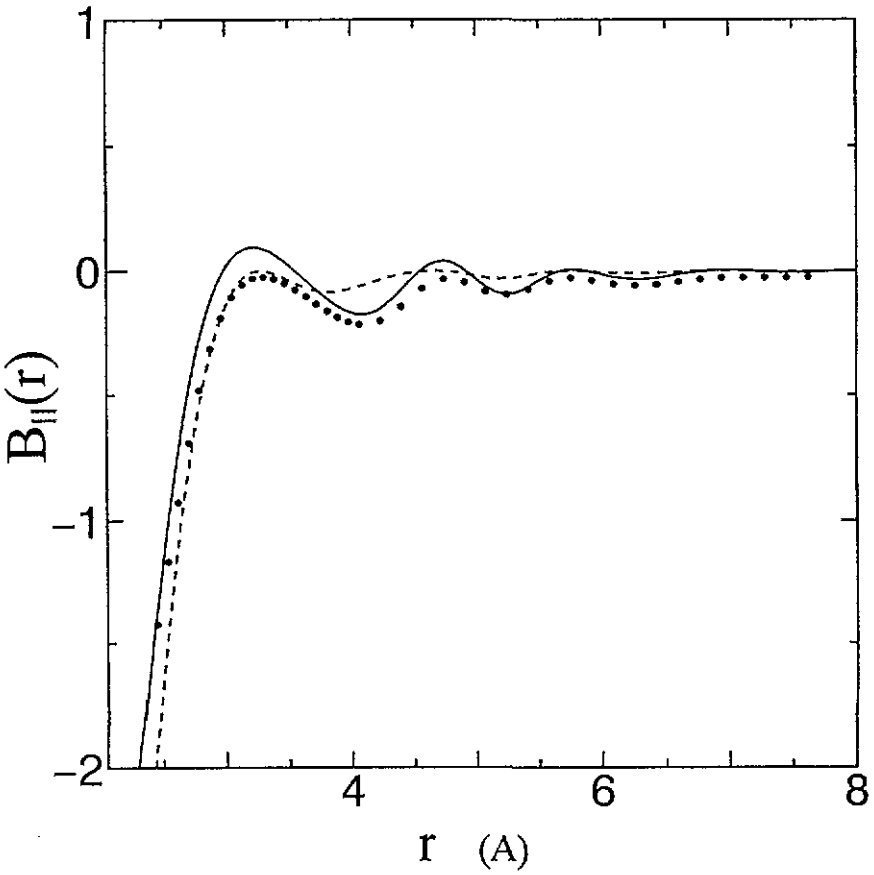

Figure 8. The bridge function for the JV-GV potential calculated by the MD method (full curve) is compared with that (full circles) of the DRT potential. The dashed curve indicates the PY bridge function with $\eta = 0.4438$

metals, where more reliable experiments are to be found. As mentioned before, the MD SF for the Ashcroft potential is close to the QHNC–MD SF as well as the MD SF for the JV potential, although their potentials differ as is shown in figure 1; the height of the first peak in the JV SF is a little lower than those of the other two SFs. In figure 4, the QHNC–MD RDF is compared with that extracted from the x-ray SF. The RDF obtained from the VMHNC equation shows a good agreement with the MD result for the QHNC potential except near the second peak, where we observe a flattening in the MD RDF as discussed by Jacucci *et al.* The reason for the Ashcroft potential producing almost the same RDF as the QHNC potential can be understood from figure 5, which shows that the core radius $r_c = 1.12a_B$ for the Ashcroft model potential yields a density distribution $\rho(r)$ of the pseudoatom close to the QHNC one except in the core region. It is interesting to find that the QHNC $\rho(r)$ has the same inner-core structure as the 3s-electron density distribution in a free Al atom.

The electron–ion RDF from the QHNC equations is shown in figure 6; its Fourier transform $S_{el}(Q)$ is represented in the form [2]

$$S_{el}(Q) = \frac{\rho(Q)}{\sqrt{Z_I}} S_{II}(Q) \tag{19}$$

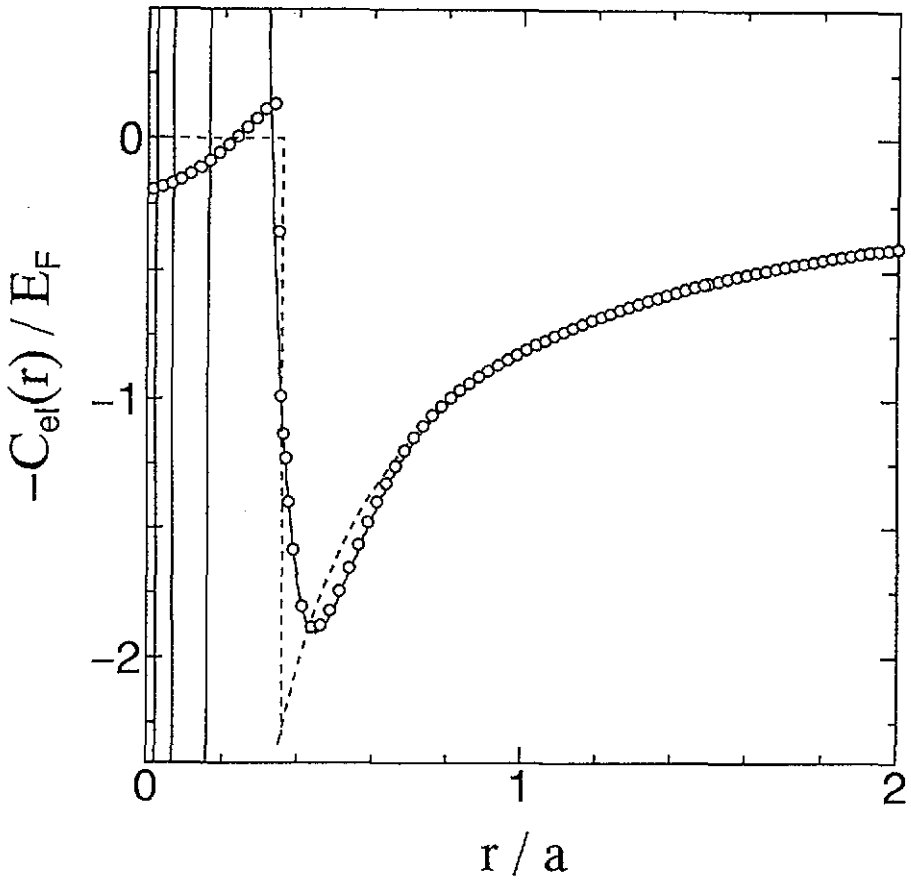

Figure 9. The pseudopotential determined by the JV method (full curve) compared with the Ashcroft model potential (dashed curve) in units of the Fermi energy E_F.

using the structure factor and the density distribution of the pseudoatom:

$$\rho(Q) \equiv \frac{n_0^e C_{eI}(Q)\chi_Q^0}{1 - n_0^e C_{ee}(Q)\chi_Q^0} . \tag{20}$$

With the help of the above equations, the pseudopotential method using the Ashcroft model potential can be used to evaluate the electron–ion RDF by inserting it into (20) instead of $-C_{eI}(r)/\beta$; the result has no inner-core structure near the origin, as is expected.

Usually, the structure factor of a liquid metal, measured by x-ray methods, is extracted by assuming that a liquid metal can be taken as an assembly of neutral atoms with the atomic form factor $f_A(Q) \equiv f_I(Q) + f_{3s}(Q)$, where $f_I(Q)$ and $f_{3s}(Q)$ are the form factors of ion and 3s valence electrons in a free atom, respectively. In reality, a liquid metal is composed of ions and conduction electrons. Due to the presence of conduction electrons, the structure factor $S_x(Q)$ extracted from x-ray data using the standard analysis shows a difference from $S_{II}(Q)$ as follows:

$$S_x(Q) = [f_M(Q)/f_A(Q)]^2 S_{II}(Q) \tag{21}$$

where $f_M(Q) = f_I(Q) + \rho(Q)$ is the form factor of a neutral pseudoatoms [24]. Since $\rho(Q)$ is very close to $f_{3s}(Q)$ as shown in figure 5, the difference between S_x and $S_{II}(Q)$,

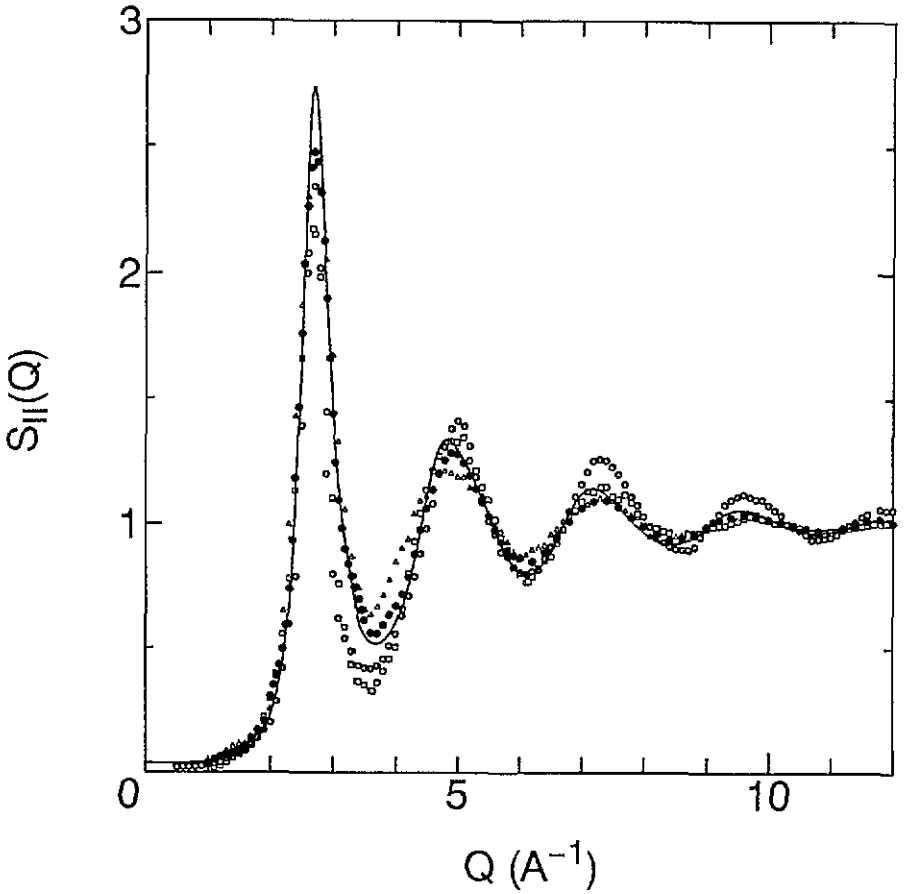

Figure 10. Comparison of various experimental structure factors: Waseda (full circles) [22], Jovic *et al* (open circles) [23], Takeda *et al* (squares) [25], and Stallard and Davis (triangles) [26]. The full curve denotes the QHNC calculation.

that is, between the x-ray and neutron diffraction SFs is very small. We have calculated the factors $[f_M(Q)/f_A(Q)]^2$ for liquid alkali metals and aluminium; the value for aluminium is at most 1% near the first peak of the SF. On the basis of the formula (21), Takeda *et al* [25] have obtained the electron–ion RDF $g_{eI}(r)$ from the analysis of the difference between the x-ray and neutron diffraction SFs, which is plotted as open circles. To obtain a reliable electron–ion RDF from this difference, it is necessary to perform the x-ray and neutron experiments with more precision and to extract the experimental structure factor with more careful error analysis, since this difference is very small as mentioned above. In figure 7, the DCFs for the JV-GV and DRT potentials are plotted together with their potentials; the DCFs show a large difference between the JV and DRT potentials. However, the bridge function for the JV potential is rather close to that for the DRT potential as shown in figure 8: the dashed curve denotes the hard-sphere bridge function with $\eta = 0.4438$ determined by the VMHNC equation.

4. Discussion

The Ashcroft model potential with $r_c = 1.12a_B$ generates the pseudoatom density $\rho(r)$ in good correspondence with that from the QHNC formulation taking account of the non-linear effect, though it has only one parameter r_c to be adjusted. In contrast to this, the DRT potential is determined in such a way as to fit the non-linear $\rho(r)$ using the non-local model potential with many parameters. However, it has a similar nature to the Ashcroft model potential in the sense that the Coulomb potential is cut off to give a constant value in the core region, like a step function; both pseudopotentials yield effective interatomic potentials with a positive minimum, if the LFC is chosen to be that of Geldart and Taylor or to be of LDA type. On the other hand, the JV pseudopotential $w_b(r) = -\beta C_{el}(r)$ with use of the LDA $G(Q)$ does not give a positive minimum in its interatomic potential (the JV-LDA potential) as seen in figure 1, although the JV method is essentially the same method as that of DRT. This difference comes from the fact that the JV pseudopotential (full curve in figure 9) deviates significantly from the Ashcroft model potential near r_c. The JV pseudopotential has an inner-core structure. Even if this is pseudized as shown by the open circles in figure 9, it generates almost the same effective interatomic potential. Thus, we can say that the positive minimum in the DRT potential may have its origin in the special functional form assumed in the non-local pseudopotential to produce the pseudoatom density. In fact, the interatomic potentials for Al calculated by Manninen *et al* [28] and Perrot [20], who used essentially the same method as DRT did, have no positive minimum and become identical to our potential with the LDA $G(Q)$. However, the MD method using the JV-LDA potential with a shallow negative potential does not give a structure factor that coincides with the experimental result; the situation is same for the Ashcroft-LDA and QHNC-LDA potentials, which yield almost the same structure factor as the case of the JV-LDA potential. We have used the GV $G(Q)$ to calculate correlations in alkali metals (Li, Na, K, Rb, Cs), and obtained structure factors in excellent agreement with experiments [27]. In alkali metals, what kind of LFC is chosen is not important; choosing either the GV or LDA $G(Q)$s produces no significant difference in the RDF, although the effective interatomic potentials differ. However, the situation is quite different in the case of a liquid metal with many valence electrons such as Al: the structure factor calculated using the LDA $G(Q)$ is significantly different from that calculated using the GV $G(Q)$, which leads to good agreement with the experimental result. This difference between the behaviours of liquid alkali metals and aluminium may be attributed to the difference between their ionic charges; the ion–ion Coulomb interaction of aluminium is larger by factor of 3^2 than that of liquid sodium. The large ionic charge of aluminium is screened by three valence electrons for each ion; the long- and intermediate-range part of the aluminium potential between ions remains very large compared to that of the sodium effective potential.

In our QHNC–MD formulation, the LFC is introduced externally in addition to the exchange–correlation potential $\mu_{XC}(n)$. The LFC in the QHNC formulation is precisely that of the electron–ion mixture defined in the electron–electron DCF $C_{ee}(Q) = -\beta v_{ee}^c(Q)[1 - G(Q)]$, which depends on the ionic structure. In the case of aluminium, where it is significantly dependent on the choice of the LFC—in contrast with the case for the alkali metals—it is important to determine the LFC $G(Q)$ via an equation coupled to the liquid structure, as was done for liquid metallic hydrogen [29, 30].

Our calculated structure factor of Al does not show such close agreement as was achieved for alkali metals. On the other hand, four experimental data sets [22, 23, 25, 26] of structure factors near the melting point deviate substantially from each other as shown in figure 10. The X-ray SFs should almost coincide with the neutron diffraction SFs, even

if the x-ray data are analysed to extract the SFs neglecting the presence of the conduction electrons as was mentioned in section 3. To compare theory with experiment, we need more accurate experiments, while the theoretical approaches also have some points that require improvement.

Acknowledgments

We would like to thank the Computing and Information Systems Centre of the Japan Atomic Energy Research Institute (JAERI) for permitting us almost unlimited use of the dedicated vector parallel processor Monte-4.

References

[1] Chihara J 1984 *J. Phys. C: Solid State Phys.* **17** 1633
[2] Chihara J 1985 *J. Phys. C: Solid State Phys.* **18** 3103
[3] Chihara J 1989 *Phys. Rev.* A **40** 4507
[4] Chihara J 1991 *J. Phys.: Condens. Matter* **3** 8715
[5] Ishitobi M and Chihara J 1992 *J. Phys.: Condens. Matter* **4** 3679
[6] Ishitobi M and Chihara J 1993 *J. Phys.: Condens. Matter* **5** 4315
[7] Ebbsjö I, Kinell T and Waller J 1980 *J. Phys. C: Solid State Phys.* **13** 1865
[8] Jacucci G, Taylor R, Tenenbaum A and van Doan N 1981 *J. Phys. F: Met. Phys.* **11** 783
[9] Bretonnet J L and Regnaut C 1985 *Phys. Rev.* B **31** 5071
[10] Hafner J and Jank W 1990 *Phys. Rev.* B **42** 11530
[11] Dagens L, Rasolt M and Taylor R 1975 *Phys. Rev.* B **11** 2726
[12] Chihara J and Ishitobi M 1994 *Mol. Simul.* **12** 1875
[13] Rosenfeld Y and Ashcroft N W 1979 *Phys. Rev.* A **20** 1208
[14] Rosenfeld Y 1986 *J. Stat. Phys.* **42** 437
[15] Geldart D J W and Vosko J H 1966 *Can. J. Phys.* **44** 2137
[16] Gunnarsson O and Lundqvist B I 1976 *Phys. Rev.* B **13** 4243
[17] Hoover W G, Ladd A J C and Moran B 1982 *Phys. Rev. Lett.* **48** 1818
[18] Kambayashi S and Chihara J 1994 *Phys. Rev.* E **50** 1317
[19] Perrot F 1990 *Phys. Rev.* A **42** 4871
[20] Perrot F and Chabrier G 1991 *Phys. Rev.* A **43** 2879
[21] Reatto L, Levesque D and Weis J J 1986 *Phys. Rev.* A **33** 3451
[22] Waseda Y 1980 *The Structure of Non-crystalline Materials* (New York: McGraw-Hill)
[23] Jovic D, Padureanu I and Rapeanu S 1977 *Inst. Phys. Conf. Ser. 30* (Bristol: Institute of Physics) p 120
[24] Chihara J 1987 *J. Phys. F: Met. Phys.* **17** 295
[25] Takeda S, Harada S, Tamaki S and Waseda Y 1991 *J. Phys. Soc. Japan* **60** 2241
[26] Stallard J M and Davis C M 1973 *Phys. Rev.* A **8** 368
[27] Kambayashi S and Chihara J, unpublished
[28] Manninen M, Jena P, Nieminen R M and Lee J K 1981 *Phys. Rev.* B **24** 7059
[29] Chihara J 1984 *Prog. Theor. Phys.* **72** 940
[30] Chihara J 1986 *Phys. Rev.* A **33** 2575